PROCEEDINGS OF SCIENCE

Lattice QCD determination of unpolarized TMDPDFs of the nucleon

Qi-An Zhang,[a,*] **Jin-Chen He,**[b,c,d] **Min-Huan Chu,**[b,c] **Jun Hua,**[e,f] **Xiangdong Ji,**[d] **Andreas Schäfer,**[g] **Yushan Su,**[d] **Wei Wang,**[c,h] **Yi-Bo Yang**[i,j,k,l] **and Jian-Hui Zhang**[m,n]

[a] *School of Physics, Beihang University, Beijing 102206, China*
[b] *Yang Yuanqing Scientific Computering Center, Tsung-Dao Lee Institute, Shanghai Jiao Tong University, Shanghai 200240, China*
[c] *Shanghai Key Laboratory for Particle Physics and Cosmology, Key Laboratory for Particle Astrophysics and Cosmology (MOE), School of Physics and Astronomy, Shanghai Jiao Tong University, Shanghai 200240, China*
[d] *Department of Physics, University of Maryland, College Park, MD 20742, USA*
[e] *Guangdong Provincial Key Laboratory of Nuclear Science, Institute of Quantum Matter, South China Normal University, Guangzhou 510006, China*
[f] *Guangdong-Hong Kong Joint Laboratory of Quantum Matter, Southern Nuclear Science Computing Center, South China Normal University, Guangzhou 510006, China*
[g] *Institut für Theoretische Physik, Universität Regensburg, D-93040 Regensburg, Germany*
[h] *Southern Center for Nuclear-Science Theory (SCNT), Institute of Modern Physics, Chinese Academy of Sciences, Huizhou 516000, Guangdong Province, China*
[i] *CAS Key Laboratory of Theoretical Physics, Institute of Theoretical Physics, Chinese Academy of Sciences, Beijing 100190, China*
[j] *School of Fundamental Physics and Mathematical Sciences, Hangzhou Institute for Advanced Study, UCAS, Hangzhou 310024, China*
[k] *International Centre for Theoretical Physics Asia-Pacific, Beijing/Hangzhou, China*
[l] *School of Physical Sciences, University of Chinese Academy of Sciences, Beijing 100049, China*
[m] *School of Science and Engineering, The Chinese University of Hong Kong, Shenzhen 518172, China*
[n] *Center of Advanced Quantum Studies, Department of Physics, Beijing Normal University, Beijing 100875, China*

E-mail: zhangqa@buaa.edu.cn

We present a first calculation of the unpolarized nucleon's isovector transverse-momentum-dependent parton distribution functions (TMDPDFs) from lattice QCD, which are essential to predict observables of multi-scale, semi-inclusive processes in the standard model. We use a $N_f = 2 + 1 + 1$ MILC ensemble with valence clover fermions on a highly improved staggered quark (HISQ) sea to compute the quark momentum distributions in a large-momentum nucleon on the lattice. The state-of-the-art techniques in renormalization and extrapolation in the correlation distance on the lattice are adopted. The perturbative kernel up to next-to-next-to-leading order is taken into account, and the dependence on the pion mass and the hadron momentum is explored. Our results are qualitatively comparable with phenomenological TMDPDFs, which provide an opportunity to predict high energy scatterings from first principles.

10th International Conference on Quarks and Nuclear Physics (QNP2024)
8-12 July, 2024
Barcelona, Spain

*Speaker

PoS(QNP2024)052

1. Introduction

Since the nucleon is at the core of atoms and accounts for nearly all of the mass of the visible universe, exploring its internal structure has been a key task for more than a century in both particle and nuclear physics. In high-energy scattering, the quark and gluon transverse momentum and polarization degrees of freedom in the nucleon are best described by transverse-momentum parton distribution functions (TMDPDFs). Thus, mapping out the nucleon's TMDPDFs is a crucial step in understanding the interactions between quarks and gluons, and possibly the phenomenon of confinement [1, 2]. Moreover, predicting the observables in multi-scale, non-inclusive high energy processes such as semi-inclusive deep-inelastic scattering and Drell-Yan scattering at the large hadron collider (LHC) or electron ion collider (EIC) heavily relies on the knowledge of TMDPDFs [3, 4].

Whereas high energy experiments have accumulated a wealth of relevant data, our knowledge of TMDPDFs is far from being complete. Their rapidity evolution, i.e. the Collins-Soper kernel [1], has been perturabtively calculated up to four loops [5, 6], but TMDPDFs at low energies are non-perturbative in nature. Based on thousands of data points from the low-p_T semi-inclusive DIS and Drell-Yan scattering processes and perturbative-QCD factorization, a number of phenomenological analyses have been made to obtain state-of-art TMDPDFs [7–11]. Although similar sets of data have been used in these analyses, the results differ significantly from each other. It indicates that significant uncertainties exist in the global extraction of TMDPDFs, and further constraints are necessary for a refined determination.

First-principles calculations of TMDPDFs require nonperturbative methods such as lattice QCD. A handful of available investigations using lattice QCD are limited to the ratios of moments of TMDPDFs [12–15]. The development of large momentum effective theory (LaMET) allows the extraction of light-cone quantities through the simulation of equal-time quasi distributions [16, 17]. A direct generalization of this essence to calculating TMDPDFs is non-trivial due to the presence of the soft function [18], which involves two opposite light-like directions and presents a crucial difficulty to implement on a Euclidean lattice. Recent progress demonstrates that the rapidity-independent (intrinsic) soft function can be calculated from a large-momentum-transfer form factor of a light meson [19], while the rapidity evolution kernel in soft function can be accessed via the quasi TMDPDFs/beam functions [18, 20–22] or quasi transverse-momentum-dependent wave functions [19, 23]. Subsequent lattice efforts have been devoted to exploring the Collins-Soper kernel and intrinsic soft function. The agreement between lattice results and phenomenological analyses is encouraging [21, 24–27].

Following these developments, this work presents a first calculation of TMDPDFs from first principles. We simulate the TMD momentum distributions in a large momentum nucleon or quasi TMDPDFs on the lattice and perform a systematic study of renormalization property by considering the subtractions from Wilson loop combined with the short distance hadron matrix element [28]. In the matching from quasi TMDPDFs, we include one-loop and two-loop perturbative contributions and employ the renormalization group equation to resum the logarithms. After analyzing the valence pion mass and momentum dependence, our final results for TMDPDFs are found to have a similar behavior as phenomenological fits.

2. Theoretical framework

Describing the momentum distributions of a parton inside a hadron, TMDPDFs $f(x, b_\perp, \mu, \zeta)$ are functions of the longitudinal momentum fraction x, the Fourier conjugate $b_\perp$ of the parton

transverse momentum $q_\perp$, as well as the renormalization scale μ and the rapidity scale ζ. In this work we will consider the flavor non-singlet/isovector unpolarized quark TMDPDFs, which do not mix with gluons.

In LaMET, the correlations with modes traveling along the light-cone can be extracted from distributions in a fast-moving nucleon through large-momentum expansion. On the lattice, the equal-time quasi TMDPDFs are constructed as

$$\tilde{f}_\Gamma\left(x, b_\perp, P^z, \mu\right) \equiv \lim_{\substack{a\to 0\\ L\to\infty}} \int \frac{dz}{2\pi} e^{-iz(xP^z)} \frac{\tilde{h}^0_\Gamma\left(z, b_\perp, P^z, a, L\right)}{\sqrt{Z_E\left(2L+z, b_\perp, a\right)} Z_O\left(1/a, \mu, \Gamma\right)}, \tag{1}$$

where a denotes the lattice spacing. $\Gamma = \gamma^t$ or γ^z is the Dirac matrix that can be projected onto γ^+ in the large momentum limit. The $\tilde{h}^0_\Gamma\left(z, b_\perp, P^z, a, L\right)$ is built with a gauge-invariant nonlocal quark bilinear operator as

$$\tilde{h}^0_\Gamma\left(z, b_\perp, P^z, a, L\right) = \langle P^z | \tilde{O}^0_{\Gamma,\sqsubset}(z, b_\perp, P^z; L) | P^z \rangle, \tag{2}$$

$$\tilde{O}^0_{\Gamma,\sqsubset}(z, b_\perp, L) \equiv \bar{\psi}(b_\perp \hat{n}_\perp) \Gamma U_{\sqsubset,L}\left(b_\perp \hat{n}_\perp, z\hat{n}_z\right) \psi(z\hat{n}_z). \tag{3}$$

In the above, $|P^z\rangle$ denotes the unpolarized nucleon state and L denotes the "infinity" that the gauge link can reach. The staple-shaped Wilson link is chosen as

$$\begin{aligned} U_{\sqsubset,L}\left(b_\perp \hat{n}_\perp, z\hat{n}_z\right) \equiv & U_z^\dagger\left((z+L)\hat{n}_z + b_\perp \hat{n}_\perp, b_\perp \hat{n}_\perp\right) U_\perp\left((z+L)\hat{n}_z + b_\perp \hat{n}_\perp, (z+L)\hat{n}_z\right) \\ & \times U_z\left((z+L)\hat{n}_z, z\hat{n}_z\right), \end{aligned} \tag{4}$$

in which U_z is the path-ordered Euclidean gauge link along the z-direction, and $U_\perp$ is along the transverse direction at the "infinity" position $(z+L)$ on the finite lattice. The staple-shaped Wilson link is depicted as double lines in Fig. 1.

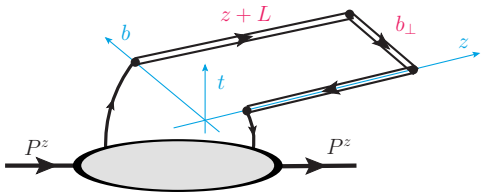

Figure 1: Illustration of the unsubtracted quasi TMDPDFs.

Quantities in Eq. (2) and (3) with the superscript "0" are bare quantities on a finite lattice. They contain linear divergence, pinch-pole singularity and logarithm divergence. Both the linear divergence and pinch-pole singularity can be renormalized by the square root of Wilson loop $\sqrt{Z_E(2L+z, b_\perp, a)}$ [29–33]; and the logarithm divergence can be renormalized by a factor $Z_O(1/a, \mu)$, which is extracted from matching between the lattice and perturbative calculation of zero-momentum matrix elements in the perturbative region [28, 34–36].

It has been shown that quasi TMDPDFs have the same collinear degree of freedoms as TMDPDFs [22]. Their differences from soft modes can be attributed to the intrinsic soft function and different rapidity scales, and meanwhile contributions from highly off-shell modes are local [20]. Thus TMDPDFs $f\left(x, b_\perp, \mu, \zeta\right)$ can be connected with quasi TMDPDFs $\tilde{f}_\Gamma\left(x, b_\perp, \zeta_z, \mu\right)$ via a multiplicative factorization [22, 37]:

$$\tilde{f}_\Gamma\left(x, b_\perp, \zeta_z, \mu\right) \sqrt{S_I\left(b_\perp, \mu\right)} = H\left(\frac{\zeta_z}{\mu^2}\right) e^{\frac{1}{2}\ln\left(\frac{\zeta_z}{\zeta}\right) K(b_\perp, \mu)} f\left(x, b_\perp, \mu, \zeta\right) + O\left(\frac{\Lambda^2_{\rm QCD}}{\zeta_z}, \frac{M^2}{(P^z)^2}, \frac{1}{b_\perp^2 \zeta_z}\right), \tag{5}$$

where S_I denotes the intrinsic soft function that has been calculated on the lattice in Refs. [25, 26, 38, 39] and K denotes the Collins-Soper kernel. The matching kernel H, as a function of $\zeta_z/\mu^2 = (2xP^z)^2/\mu^2$, has been perturbatively determined up to the next-to-next-to-leading order (NNLO) [20, 22, 40–43]. Power corrections are suppressed by $O\left(\Lambda^2_{\rm QCD}/\zeta_z, M^2/(P^z)^2, 1/(b_\perp^2\zeta_z)\right)$, which implies that TMDPDFs can only be accurately obtained in the moderate range of x.

3. Lattice simulations

We use the valence tadpole improved clover fermion on the hypercubic (HYP) smeared [44] $2+1+1$ flavors MILC configurations with highly improved staggered quark (HISQ) sea and 1-loop Symanzik improved gauge action [45]. This calculation uses a single ensemble with lattice spacing $a = 0.12$ fm and volume $n_s^3 \times n_t = 48^3 \times 64$, physical sea quark masses, and two choices of light valence quark mass corresponding to $m_\pi^{\rm val} = \{220,\ 310\}$ MeV. HYP smearing is also used for nonlocal correlation functions to improve the statistical signal. In order to explore the momentum dependence, we employ three different nucleon momenta $P^z = 2\pi/(n_s a)\times\{8, 10, 12\} = \{1.72, 2.15, 2.58\}$ GeV.

We adopt momentum-smearing point sources [46] on several time slices, and average correlation functions for both the forward and backward directions in z and transverse space of the gauge link. In total, there are 1000 (configurations) $\times$16 (source time slices) $\times$4 (forward/backward directions of the z and transverse axes) measurements for the $m_\pi^{\rm val} = 220$ MeV case and $1000\times4\times4$ measurements for the 310 MeV case.

To extract the quasi TMDPDFs, one constructs the two- and three-point functions as

$$C_2(t) = \left\langle \sum_{\vec{y}} e^{i\vec{P}\cdot\vec{y}} T\chi(\vec{y},t)\bar{\chi}(\vec{0},0)\right\rangle, \tag{6}$$

$$C_3^\Gamma(t,t_s) = \left\langle \sum_{\vec{y}} e^{i\vec{P}\cdot\vec{y}} T\chi(\vec{y},t_s) \sum_{\vec{x}} \tilde{O}^\Gamma_{\rm TMD}(\vec{x},t)\,\bar{\chi}(\vec{0},0)\right\rangle, \tag{7}$$

where $T = (1+\gamma^t)/2$ denotes the unpolarized projector, and $\chi = \epsilon^{abc} u_a \left(u_b^T C\gamma_5 d_c\right)$ is the nucleon interpolation field. We adopt the sequential source method [47] to reduce the number of propagators in 3pt functions, t_s denotes the time position of the sequential source. The operator $\tilde{O}^\Gamma_{\rm TMD}(\vec{x},t)$ is short for the TMD nonlocal quark bilinear operator $\tilde{O}^0_\sqsubset(\vec{x}+z\hat{n}_z, \vec{x}+b_\perp\hat{n}_\perp, \Gamma, L)$ at discrete time slice $t \in [0, t_s]$. The three-momentum is chosen as $\vec{P} = (0,0,P^z)$.

For a well-defined quasi TMDPDF, the length of Wilson link L should be large enough to ensure that the final results are independent of L. Here we adopt $L = 6a$, which is also in line with Ref. [28]. After inserting the single particle intermediate states, one can parametrize the ratio as

$$\frac{C_3^\Gamma(t,t_s)}{C_2(t_s)} = \frac{\tilde{h}^0_\Gamma + c_2\left(e^{-\Delta E t} + e^{-\Delta E(t_s-t)}\right) + c_3 e^{-\Delta E t_s}}{1 + c_1 e^{-\Delta E t_s}}, \tag{8}$$

in which $\tilde{h}^0_\Gamma \equiv \tilde{h}^0(z, b_\perp, P^z, \Gamma)$, ΔE is the mass gap between the ground-state and excited state, and $c_{1,2,3}$ are parameters for the excited-state contaminations. Combing the parametrization form of 2pt functions: $C_2(t) = c_0 e^{-E_0 t}\left(1 + c_1 e^{-\Delta E t}\right)$, one can extract the values of $\tilde{h}^0_\Gamma$ at fixed $(z, b_\perp, P^z)$ through a correlated joint fit. In our calculation, we use bootstrap resampling to establish correlations among all datasets, and the correlations are maintained consistently throughout the entire analysis. By implementing fully correlated Bayesian constrained fits, we obtain the ground state matrix elements.

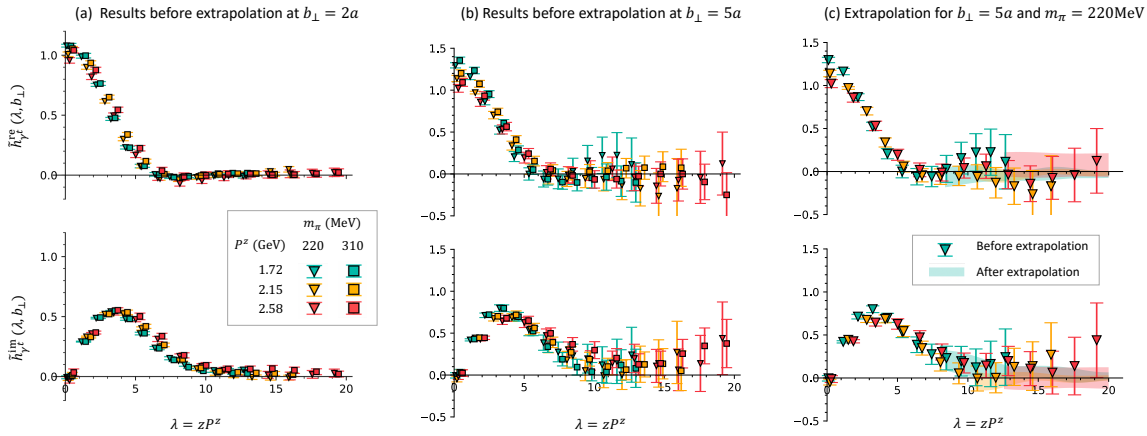

Figure 2: (a, b): Renormalized matrix elements as function of $\lambda = zP^z$ with various m_π and P^z at $b_\perp = 2a$ and $5a$; (c): Comparison of original lattice (data points) and extrapolated results (colored bands) at $b_\perp = 5a$.

Combining the bare quasi TMDPDFs matrix elements with the corresponding Wilson loop and renormalization factor, we obtain numerical results for renormalized matrix elements at different $\lambda = zP^z$. The two panels on the left in Fig. 2 exhibit the λ dependence of the renormalized matrix elements with $b_\perp = 2a$ and $5a$ with various P^z and m_π. It can be seen that as λ increases, the quasi TMDPDFs approach zero for both real and imaginary components. When $b_\perp$ is large, considerable uncertainties exist in the fully correlated datasets and non-zero central values can induce unphysical oscillations for a brute-force Fourier transformation. To address this problem, we adopt a physics-inspired extrapolation at large λ: [32]

$$\tilde{h}_{\Gamma,\text{extra}}(\lambda) = \left[\frac{m_1}{(-i\lambda)^{n_1}} + e^{i\lambda}\frac{m_2}{(i\lambda)^{n_2}}\right] e^{-\lambda/\lambda_0}, \tag{9}$$

in which all parameters $m_{1,2}$, $n_{1,2}$ and λ_0 depend on the transverse separation $b_\perp$. The algebraic terms account for a power law behavior of TMDPDFs in the endpoint region, and the exponential term is motivated by the expectation that the correlation function has a finite correlation length (denoted as λ_0) [32] at finite momentum.

To perform the extrapolation, a reasonable range of λ is required to determine the parameters. We choose the lattice data at $z \geq 8a$ for the extrapolation, and vary it down to $6a$ to estimate the systematic errors. As shown in Fig. 2(c), the extrapolated results (colored bands) agree with lattice data in the moderate λ region, and give smoothly-decaying distributions at large λ.

After the Fourier transformation, one can obtain the quasi TMDPDF $\tilde{f}_\Gamma(x, b_\perp, \zeta_z, \mu)$, shown as the dashdotted (magenta) line in Fig. 3. Combing the updated results of Collins-Soper kernel [27] and intrinsic soft function [39] calculated on the same ensembles, we obtain the TMDPDFs through the matching formula in Eq.(5). Fig. 3 shows an example of matched TMDPDF from the NLO [22, 41] and NNLO [42, 43] kernel with RG running to scale $\mu = \sqrt{\zeta} = 2$ GeV. One can see that the results agree within uncertainties, except for the endpoint region.

4. Physical extrapolation and error estimation

It should be noted that the TMDPDFs can be obtained after employing the factorization formula, while residual dependence on the lattice inputs (such as P^z and m_π) may still reside in the obtained

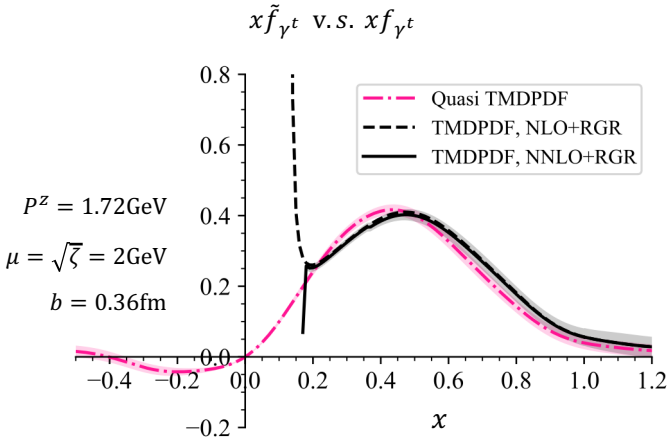

Figure 3: Quasi TMDPDF (dashed-red line) with nucleon boosted momentum $P^z = 1.72$ GeV and matched TMDPDF from NLO kernel (dashed-black line, no error) and NNLO kernel (solid-black line) with RG running to scale $\mu = \sqrt{\zeta} = 2$ GeV at $b_\perp = 3a$. Only statistical errors are included in the bands. Deviations between NLO and NNLO results at $x < 0.2$ indicate that the perturbative matching fails in small-x region.

results. To diminish the dependence, we extrapolate the above results to the physical m_π value (135 MeV) and infinite momentum using the following ansatz:

$$f(m_\pi, P^z) = f_{\text{phy}}\left[1 + d_0\left(m_\pi^2 - m_{\pi,\text{phy}}^2\right) + d_0' \ln(m_\pi^2/m_{\pi,\text{phy}}^2) + \frac{d_1}{(P^z)^2} + \frac{d_1'}{P^z}\right], \quad (10)$$

where the $d_0^{(\prime)}$ term characterizes the pion mass dependence, and $d_1^{(\prime)}$ accounts for the momentum-dependent discretization error. Taking $d_0' = d_1' = 0$ as our default case, we obtain the physical TMDPDF from a joint fit of $f(m_\pi, P^z)$. To explore the systematic bias in the extrapolation ansatz, we estimate the m_π dependence by using the d_0' term (with $d_0 = 0$) and examine the $1/P^z$ contributions by adding the d_1' term. We include their differences in the systematic uncertainties.

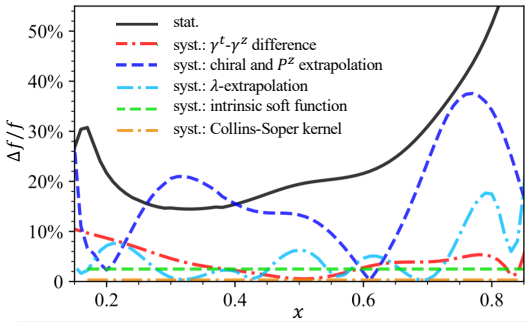

Figure 4: Ratios of various uncertainties and central value of final TMDPDF at $b_\perp = 3a$, include the statistical one and systematical one from: (1) $\gamma^t - \gamma^z$ differences, (2) chiral and P^z extrapolation, (3) λ extrapolation, (4) intrinsic soft function [39] and (5) Collins-Soper kernel [27].

In quasi TMDPDFs, both Lorentz structures $\Gamma = \gamma^t, \gamma^z$ can project onto γ^+ in the large momentum limit. In this work we have used γ^t to extract the TMDPDFs, while it has been noticed that the γ^t case has less operator mixing effects [48]. For the γ^z case, in addition to operator mixing

effects, its difference with the γ^t case may come from remnant power corrections. As an estimate, we take this difference as a systematic uncertainty.

Besides the statistical uncertainties, this work considers systematic errors from different sources, shown in Fig. 4. They arise from the difference between the γ^t and γ^z results, different strategies for the chiral and P^z extrapolation, and different fitting ranges in the λ-extrapolation. In addition, we consider the error propagating from the intrinsic soft function [39] and Collins-Soper kernel [27], which are calculated on the same configurations. We did our best to estimate systematic uncertainties, but cannot exclude that there exist others, potentially important ones.

5. Numerical results

Combing all the known uncertainties indicated in Fig. 4, we obtain numerical results of unpolarized nucleon's isovector TMDPDFs from our lattice simulation. Fig. 5 shows $xf(x, b_\perp, \mu, \zeta)$ at renormalization and rapidity scales $\mu = \sqrt{\zeta} = 2$ GeV as a function of x, together with the phenomenological results from global analyses [7–11]. From the comparison one can see that, our results are in qualitative agreement with phenomenological results and share similar behaviors in $b_\perp$ space: the central values slowly decrease and uncertainties are gradually increasing with the increase of $b_\perp$.

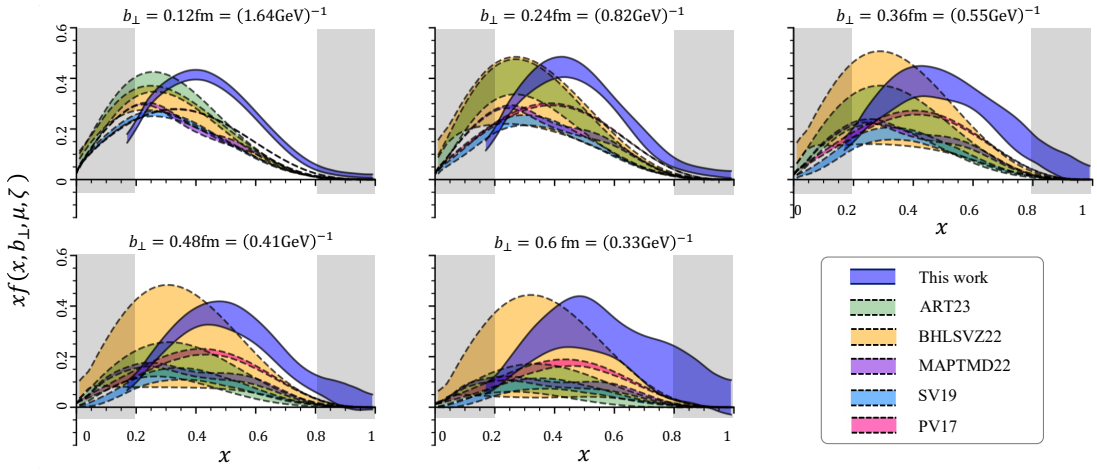

Figure 5: Our final results for unpolarized nucleon's isovector TMDPDFs $xf(x, b_\perp, \mu, \zeta)$ at renormalization and rapidity scales at $\mu = \sqrt{\zeta} = 2$ GeV, extrapolated to physical pion mass 135 MeV and infinite momentum limit $P^z \to \infty$, compared with ART23 [7], BHLSVZ22 [8], MAPTMD22 [9], SV19 [10]and PV17 [11] global fits. The colored bands denote our results with both statistical and systematic uncertainties, the shaded grey regions imply the endpoint regions where LaMET predictions are not reliable.

The two shaded bands at the endpoint regions ($x < 0.2$ and $x > 0.8$) in each subplots of Fig. 5 indicate that LaMET predictions are not reliable there, which is estimated from the power correction terms $\Lambda^2_{\text{QCD}}/(xP^z)^2$ and threshold logarithms $\ln((1-x)P^z)$ [49, 50] . Besides, since only one lattice spacing is used, discretization uncertainties are not properly handled at this stage. Especially the $b_\perp \sim a$ case might suffer sizable discretization effects, which can be improved by a more detailed analysis in future.

Fig. 6 shows the results $xf(x, b_\perp, \mu, \zeta)$ with $x = 0.3, 0.5, 0.7$ as a function of spatial separation $b_\perp$. The spatial distributions reflect correlations between the partons at transverse interval $b_\perp$ inside a highly boosted nucleon, and will reveal aspects of nucleon structure. It could be conjectured that

the distributions vanish when $b_\perp$ is larger than the nucleon radius, however, neither the lattice nor the phenomenological results are precise enough to draw such a conclusion now.

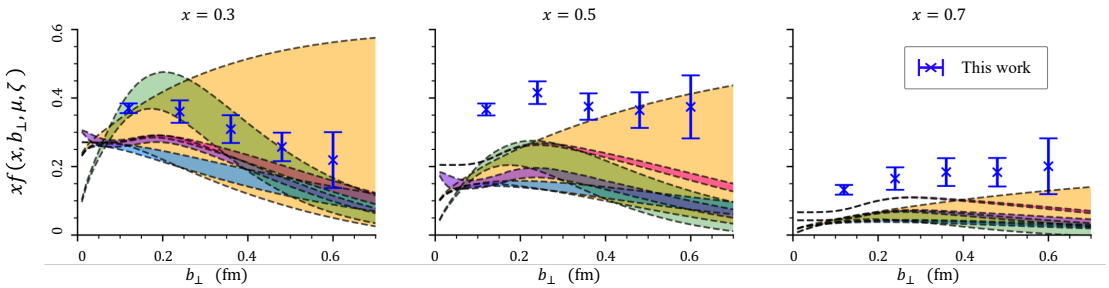

Figure 6: The TMDPDFs $xf(x, b_\perp, \mu = 2\ \text{GeV}, \zeta = 4\ \text{GeV}^2)$ with longitudinal momentum fraction $x = \{0.3, 0.5, 0.7\}$, together with the phenomenological results. The labels of latter are same as Fig. 5.

6. Summary and Prospect

In summary, we have presented a first calculation of TMDPDFs inside a nucleon using LaMET expansion of the lattice data. State-of-the-art techniques in renormalization and extrapolation on the lattice are adopted. The perturbative kernel up to NNLO with RG resummation is taken into account. We explore the dependence on pion mass and hadron momentum, and both statistical errors and systematic errors are included to give a reliable description of nucleons' inner structure as described by the parton distributions.

Though the final results are encouraging, further improvements are needed. Firstly a full-fledged analysis on multiple ensembles with different lattice spacings, pion masses and volumes is eagerly called for. This does not only re-investigate all the uncertainties considered in this work, but also explore other important ones in a systematic manner. Secondly, our results suffer from sizable theoretical uncertainties in endpoint regions, which may come from power corrections or threshold logarithms. Thirdly, we anticipate a decaying behavior for the $b_\perp$ distribution in the tomography of the nucleon. To validate this expectation, a sufficiently large transverse separation is necessary. In addition, it has been noticed that chiral logarithms enter the analysis of quasi PDFs (see for instance Ref. [51]). Similar logarithms may appear in our case which requests a dedicated theoretical exploration.

7. Acknowledgements

We thank Alessandro Bacchetta, Matteo Cerutti, Alexey Vladimirov for sharing their data for this work. We also thank the MILC collaboration for providing us their gauge configurations with dynamical fermions. This work is supported in part by Natural Science Foundation of China under grant No. 11911530088, U2032102, 12005130, 12125503, 12375069. The computations in this paper were run on the Siyuan-1 cluster supported by the Center for High Performance Computing at Shanghai Jiao Tong University, and Advanced Computing East China Sub-center. The numerical calculation in this study were also carried out on the ORISE Supercomputer, and HPC Cluster of ITP-CAS. J.H. is partially support by the U.S. Department of Energy, Office of Science, Office of Nuclear Physics under the umbrella of the Quark-Gluon Tomography (QGT) Topical Collaboration with Award DE-SC0023646. X.J. and Y.S. are supported by the U.S. Department of Energy, Office

of Science, Office of Nuclear Physics, under contract number DE-SC0020682. Y.Y. is supported in part by the Strategic Priority Research Program of Chinese Academy of Sciences, Grant No. XDB34030303 and XDPB15. J.Z. is supported in part by National Natural Science Foundation of China under grant No. 11975051. A.S, W.W, Y.Y and J.Z are also supported by a NSFC-DFG joint grant under grant No. 12061131006 and SCHA 458/22. Q.Z. is supported by the Key Laboratory of Particle Astrophysics and Cosmology, Ministry of Education of China.

References

[1] J. C. Collins and D. E. Soper, Nucl. Phys. B **193**, 381 (1981) [erratum: Nucl. Phys. B **213**, 545 (1983)] doi:10.1016/0550-3213(81)90339-4

[2] R. Angeles-Martinez, A. Bacchetta, I. I. Balitsky, D. Boer, M. Boglione, R. Boussarie, F. A. Ceccopieri, I. O. Cherednikov, P. Connor and M. G. Echevarria, *et al.* Acta Phys. Polon. B **46**, no.12, 2501-2534 (2015) doi:10.5506/APhysPolB.46.2501 [arXiv:1507.05267 [hep-ph]].

[3] J. C. Collins, D. E. Soper and G. F. Sterman, Nucl. Phys. B **250**, 199-224 (1985) doi:10.1016/0550-3213(85)90479-1

[4] A. Accardi, J. L. Albacete, M. Anselmino, N. Armesto, E. C. Aschenauer, A. Bacchetta, D. Boer, W. K. Brooks, T. Burton and N. B. Chang, *et al.* Eur. Phys. J. A **52**, no.9, 268 (2016) doi:10.1140/epja/i2016-16268-9 [arXiv:1212.1701 [nucl-ex]].

[5] I. Moult, H. X. Zhu and Y. J. Zhu, JHEP **08**, 280 (2022) doi:10.1007/JHEP08(2022)280 [arXiv:2205.02249 [hep-ph]].

[6] C. Duhr, B. Mistlberger and G. Vita, Phys. Rev. Lett. **129**, no.16, 162001 (2022) doi:10.1103/PhysRevLett.129.162001 [arXiv:2205.02242 [hep-ph]].

[7] V. Moos, I. Scimemi, A. Vladimirov and P. Zurita, [arXiv:2305.07473 [hep-ph]].

[8] M. Bury, F. Hautmann, S. Leal-Gomez, I. Scimemi, A. Vladimirov and P. Zurita, JHEP **10**, 118 (2022) doi:10.1007/JHEP10(2022)118 [arXiv:2201.07114 [hep-ph]].

[9] A. Bacchetta *et al.* [MAP (Multi-dimensional Analyses of Partonic distributions)], JHEP **10**, 127 (2022) doi:10.1007/JHEP10(2022)127 [arXiv:2206.07598 [hep-ph]].

[10] I. Scimemi and A. Vladimirov, JHEP **06**, 137 (2020) doi:10.1007/JHEP06(2020)137 [arXiv:1912.06532 [hep-ph]].

[11] A. Bacchetta, F. Delcarro, C. Pisano, M. Radici and A. Signori, JHEP **06**, 081 (2017) [erratum: JHEP **06**, 051 (2019)] doi:10.1007/JHEP06(2017)081 [arXiv:1703.10157 [hep-ph]].

[12] P. Hagler, B. U. Musch, J. W. Negele and A. Schafer, EPL **88**, no.6, 61001 (2009) doi:10.1209/0295-5075/88/61001 [arXiv:0908.1283 [hep-lat]].

[13] B. U. Musch, P. Hagler, M. Engelhardt, J. W. Negele and A. Schafer, Phys. Rev. D **85**, 094510 (2012) doi:10.1103/PhysRevD.85.094510 [arXiv:1111.4249 [hep-lat]].

[14] B. Yoon, T. Bhattacharya, M. Engelhardt, J. Green, R. Gupta, P. Hägler, B. Musch, J. Negele, A. Pochinsky and S. Syritsyn, [arXiv:1601.05717 [hep-lat]].

[15] B. Yoon, M. Engelhardt, R. Gupta, T. Bhattacharya, J. R. Green, B. U. Musch, J. W. Negele, A. V. Pochinsky, A. Schäfer and S. N. Syritsyn, Phys. Rev. D **96**, no.9, 094508 (2017) doi:10.1103/PhysRevD.96.094508 [arXiv:1706.03406 [hep-lat]].

[16] X. Ji, Phys. Rev. Lett. **110**, 262002 (2013) doi:10.1103/PhysRevLett.110.262002 [arXiv:1305.1539 [hep-ph]].

[17] X. Ji, Sci. China Phys. Mech. Astron. **57**, 1407-1412 (2014) doi:10.1007/s11433-014-5492-3 [arXiv:1404.6680 [hep-ph]].

[18] X. Ji, P. Sun, X. Xiong and F. Yuan, Phys. Rev. D **91**, 074009 (2015) doi:10.1103/PhysRevD.91.074009 [arXiv:1405.7640 [hep-ph]].

[19] X. Ji, Y. Liu and Y. S. Liu, Nucl. Phys. B **955**, 115054 (2020) doi:10.1016/j.nuclphysb.2020.115054 [arXiv:1910.11415 [hep-ph]].

[20] M. A. Ebert, I. W. Stewart and Y. Zhao, JHEP **09**, 037 (2019) doi:10.1007/JHEP09(2019)037 [arXiv:1901.03685 [hep-ph]].

[21] P. Shanahan, M. Wagman and Y. Zhao, Phys. Rev. D **102**, no.1, 014511 (2020) doi:10.1103/PhysRevD.102.014511 [arXiv:2003.06063 [hep-lat]].

[22] X. Ji, Y. Liu and Y. S. Liu, Phys. Lett. B **811**, 135946 (2020) doi:10.1016/j.physletb.2020.135946 [arXiv:1911.03840 [hep-ph]].

[23] X. Ji and Y. Liu, Phys. Rev. D **105**, no.7, 076014 (2022) doi:10.1103/PhysRevD.105.076014 [arXiv:2106.05310 [hep-ph]].

[24] M. Schlemmer, A. Vladimirov, C. Zimmermann, M. Engelhardt and A. Schäfer, JHEP **08**, 004 (2021) doi:10.1007/JHEP08(2021)004 [arXiv:2103.16991 [hep-lat]].

[25] Q. A. Zhang *et al.* [Lattice Parton], Phys. Rev. Lett. **125**, no.19, 192001 (2020) doi:10.22323/1.396.0477 [arXiv:2005.14572 [hep-lat]].

[26] Y. Li, S. C. Xia, C. Alexandrou, K. Cichy, M. Constantinou, X. Feng, K. Hadjiyiannakou, K. Jansen, C. Liu and A. Scapellato, *et al.* Phys. Rev. Lett. **128**, no.6, 062002 (2022) doi:10.1103/PhysRevLett.128.062002 [arXiv:2106.13027 [hep-lat]].

[27] M. H. Chu *et al.* [LPC], Phys. Rev. D **106**, no.3, 034509 (2022) doi:10.1103/PhysRevD.106.034509 [arXiv:2204.00200 [hep-lat]].

[28] K. Zhang *et al.* [[Lattice Parton Collaboration (LPC)]], Phys. Rev. Lett. **129**, no.8, 082002 (2022) doi:10.1103/PhysRevLett.129.082002 [arXiv:2205.13402 [hep-lat]].

[29] X. Ji, J. H. Zhang and Y. Zhao, Phys. Rev. Lett. **120**, no.11, 112001 (2018) doi:10.1103/PhysRevLett.120.112001 [arXiv:1706.08962 [hep-ph]].

[30] T. Ishikawa, Y. Q. Ma, J. W. Qiu and S. Yoshida, Phys. Rev. D **96**, no.9, 094019 (2017) doi:10.1103/PhysRevD.96.094019 [arXiv:1707.03107 [hep-ph]].

[31] J. Green, K. Jansen and F. Steffens, Phys. Rev. Lett. **121**, no.2, 022004 (2018) doi:10.1103/PhysRevLett.121.022004 [arXiv:1707.07152 [hep-lat]].

[32] X. Ji, Y. Liu, A. Schäfer, W. Wang, Y. B. Yang, J. H. Zhang and Y. Zhao, Nucl. Phys. B **964**, 115311 (2021) doi:10.1016/j.nuclphysb.2021.115311 [arXiv:2008.03886 [hep-ph]].

[33] P. Shanahan, M. L. Wagman and Y. Zhao, Phys. Rev. D **101**, no.7, 074505 (2020) doi:10.1103/PhysRevD.101.074505 [arXiv:1911.00800 [hep-lat]].

[34] X. D. Ji and M. J. Musolf, Phys. Lett. B **257**, 409-413 (1991) doi:10.1016/0370-2693(91)91916-J

[35] Y. K. Huo *et al.* [Lattice Parton Collaboration (LPC)], Nucl. Phys. B **969**, 115443 (2021) doi:10.1016/j.nuclphysb.2021.115443 [arXiv:2103.02965 [hep-lat]].

[36] Y. Ji, J. H. Zhang, S. Zhao and R. Zhu, Phys. Rev. D **104**, no.9, 094510 (2021) doi:10.1103/PhysRevD.104.094510 [arXiv:2104.13345 [hep-ph]].

[37] M. A. Ebert, S. T. Schindler, I. W. Stewart and Y. Zhao, JHEP **04**, 178 (2022) doi:10.1007/JHEP04(2022)178 [arXiv:2201.08401 [hep-ph]].

[38] M. H. Chu, J. C. He, J. Hua, J. Liang, X. Ji, A. Schafer, H. T. Shu, Y. Su, J. H. Wang and W. Wang, *et al.* [arXiv:2302.09961 [hep-lat]].

[39] M. H. Chu *et al.* [Lattice Parton (LPC)], JHEP **08**, 172 (2023) doi:10.1007/JHEP08(2023)172 [arXiv:2306.06488 [hep-lat]].

[40] X. Ji, L. C. Jin, F. Yuan, J. H. Zhang and Y. Zhao, Phys. Rev. D **99**, no.11, 114006 (2019) doi:10.1103/PhysRevD.99.114006 [arXiv:1801.05930 [hep-ph]].

[41] X. Ji, Y. S. Liu, Y. Liu, J. H. Zhang and Y. Zhao, Rev. Mod. Phys. **93**, no.3, 035005 (2021) doi:10.1103/RevModPhys.93.035005 [arXiv:2004.03543 [hep-ph]].

[42] X. Ji, Y. Liu and Y. Su, [arXiv:2305.04416 [hep-ph]].

[43] Ó. del Río and A. Vladimirov, [arXiv:2304.14440 [hep-ph]].

[44] A. Hasenfratz and F. Knechtli, Phys. Rev. D **64**, 034504 (2001) doi:10.1103/PhysRevD.64.034504 [arXiv:hep-lat/0103029 [hep-lat]].

[45] A. Bazavov *et al.* [MILC], Phys. Rev. D **87**, no.5, 054505 (2013) doi:10.1103/PhysRevD.87.054505 [arXiv:1212.4768 [hep-lat]].

[46] G. S. Bali, B. Lang, B. U. Musch and A. Schäfer, Phys. Rev. D **93**, no.9, 094515 (2016) doi:10.1103/PhysRevD.93.094515 [arXiv:1602.05525 [hep-lat]].

[47] G. W. Kilcup, S. R. Sharpe, R. Gupta, G. Guralnik, A. Patel and T. Warnock, Phys. Lett. B **164**, 347-355 (1985) doi:10.1016/0370-2693(85)90339-9

[48] M. Constantinou, H. Panagopoulos and G. Spanoudes, Phys. Rev. D **99**, no.7, 074508 (2019) doi:10.1103/PhysRevD.99.074508 [arXiv:1901.03862 [hep-lat]].

[49] V. M. Braun, A. Vladimirov and J. H. Zhang, Phys. Rev. D **99**, no.1, 014013 (2019) doi:10.1103/PhysRevD.99.014013 [arXiv:1810.00048 [hep-ph]].

[50] X. Gao, K. Lee, S. Mukherjee, C. Shugert and Y. Zhao, Phys. Rev. D **103**, no.9, 094504 (2021) doi:10.1103/PhysRevD.103.094504 [arXiv:2102.01101 [hep-ph]].

[51] W. Y. Liu and J. W. Chen, Phys. Rev. D **104**, no.5, 054508 (2021) doi:10.1103/PhysRevD.104.054508 [arXiv:2011.13536 [hep-lat]].

[52] Y. Su, J. Holligan, X. Ji, F. Yao, J. H. Zhang and R. Zhang, Nucl. Phys. B **991**, 116201 (2023) doi:10.1016/j.nuclphysb.2023.116201 [arXiv:2209.01236 [hep-ph]].

[53] H. W. Lin, J. W. Chen and R. Zhang, [arXiv:2011.14971 [hep-lat]].

[54] S. Moch, B. Ruijl, T. Ueda, J. A. M. Vermaseren and A. Vogt, JHEP **10**, 041 (2017) doi:10.1007/JHEP10(2017)041 [arXiv:1707.08315 [hep-ph]].

[55] R. N. Lee, A. V. Smirnov, V. A. Smirnov and M. Steinhauser, JHEP **02**, 172 (2019) doi:10.1007/JHEP02(2019)172 [arXiv:1901.02898 [hep-ph]].

PoS(QNP2024)052